ELSEVIER

Journal of Food Engineering 51 (2002) 185–192

JOURNAL OF FOOD ENGINEERING

www.elsevier.com/locate/jfoodeng

On-line inspection of poultry carcasses by a dual-camera system

Kuanglin Chao [a,*], Yud-Ren Chen [a], William R. Hruschka [a], Frank B. Gwozdz [b]

[a] *Instrumentation and Sensing Laboratory, USDA/ARS/BARC-E, Building 303, 10300 Baltimore Avenue, Beltsville, MD 20705-2350, USA*
[b] *Food Safety and Inspection Service, USDA, Washington, DC 20250, USA*

Received 1 March 2000; received in revised form 12 August 2000; accepted 12 August 2000

Abstract

The Instrumentation and Sensing Laboratory (ISL) has developed a multi-spectral imaging system for on-line inspection of poultry carcasses. The ISL design is based on two principles: (1) wholesome and unwholesome birds have different chemical compositions of tissues and may have different skin color, and (2) unwholesome carcasses may have physical abnormalities which can be detected by computerized imaging. On-line trials of the multi-spectral chicken carcass inspection system were conducted during a 14-day period in a poultry-processing plant in New Holland, Pennsylvania, where spectral images of 13,132 wholesome and 1459 unwholesome chicken carcasses were measured. For off-line model development, the accuracies for classification of wholesome and unwholesome carcasses were 95% and 88%. On-line testing of the neural network classification models with combination of the filter information was performed. The inspection system gave accuracies of 94% and 87% for wholesome and unwholesome carcasses, respectively. This accuracy was consistent with the results obtained previously on laboratory studies. Thus, the inspection system shows promise for separation of unwholesome chicken carcasses from wholesome carcasses in poultry processing lines. Published by Elsevier Science Ltd.

Keywords: Broiler; Classification; Food safety; Machine vision

1. Introduction

The number of chickens slaughtered at federally inspected establishments has grown from three billion in the mid-1960s to roughly eight billion per year in 1995, and this quantity continues to increase (US Department of Agriculture, 1997). To meet increasing demand, some line speeds at poultry plants were increased from 70 to 91 birds per minute and more recently some plants with new automated evisceration equipment are operating at 140 birds per minute.

The USDA uses several thousand government inspectors in the Food Safety and Inspection Service (FSIS) to inspect each individual bird. Inspectors examining 30–35 chickens per minute for at least 8 h per day have a tendency to develop carpal tunnel syndrome, repetitive motion injuries, and attention and fatigue problems (OSHA, 1999).

An automated machine-based inspection system could accurately screen and separate questionable carcasses from wholesome poultry carcasses (Chen & Massie, 1993; Daley, Soulakos, Thompson, & Millet, 1988; Park & Chen, 1994). Inspectors then would only have to "re-inspect" questionable carcasses to ensure wholesome carcasses are not discarded. Chickens requiring human inspection could then be reduced by about 80–90%. A machine vision instrumental inspection system would improve inspection accuracy, increase plant output, improve overall inspection effectiveness, reduce the inspection cost per bird, and free up USDA inspectors for hazard analysis and critical control points (HACCP) functions, the new FSIS inspection program to examine critical aspects of plant processes. Also, implementing an automated poultry inspection system would provide more consumer confidence in poultry.

The Instrumentation and Sensing Laboratory (ISL) of the USDA Agricultural Research Service (ARS) in Beltsville, Maryland has developed an automated poultry inspection system. It consists of two sub-systems, a visible/near-infrared (Vis/NIR) spectrometer and a spectral imaging sub-system. ISL has shown that the Vis/NIR sub-system performs favorably in the classification of wholesome and unwholesome carcasses (Chen, Huffman, Park, & Nguyen, 1996). The overall prediction accuracy of the Vis/NIR sub-system ranges from 95% to 98% when its conclusions are compared with those of an

* Corresponding author. Tel.: +1-301-504-8450; fax: +1-301-504-9466.
E-mail address: chaok@ba.ars.usda.gov (K. Chao).

0260-8774/01/$ - see front matter. Published by Elsevier Science Ltd.
PII: S0260-8774(01)00051-6

FSIS veterinarian in a poultry process plant (Chen, Hruschka, & Earl, 2000).

The spectral imaging sub-system (Chao, Park, Chen, Hruschka, & Wheaton, 2000) uses one pair of black and white cameras with two band-pass filters (540 and 700 nm). These wavelengths were found in previous work (Park & Chen, 1994) to be optimal for detection of abnormalities. The sub-system measures the intensity of diffusely reflected light from a surface. The reflected light contains information about absorbers near the surface of the material and analysis of the images can detect physical abnormalities. In general, comparison of images at two or more wavelengths provides robustness for classifying spectral images. Since the process of analyzing a digital image to identify certain objects is inherently computationally intensive, it is advantageous to optically pre-process the image, extracting only those features that provide useful information.

Using a neural network, the sub-system can learn and predict which chickens are wholesome or unwholesome. The time it takes for the sub-system to decide whether a chicken is wholesome or not is faster than the present maximum plant production speeds of 91 birds per minute. Therefore, the sub-system can operate on the processing line and will provide a record of the condition of each bird passing by the sub-system.

On-line testing of the imaging sub-system in a plant environment was conducted at Tyson Foods (New Holland, PA) in September 1999. This paper reports the results of these trials.

2. Materials and methods

2.1. Hardware

Industrial machine frames (ParFrame, Parker automation, Wadsworth, OH) were utilized to fabricate the transportable dual-camera system. A schematic of the dual-camera system is shown in Fig. 1, and a description of its major components is given in Chao et al., 2000, which describes the laboratory version of the system.

For on-line in-plant model development and testing, the illumination described in Chao et al., 2000 was changed to a fiber-optic dual-line light (QDF5048, Dolan-Jenner Industries, Lawrence, MA) equipped with AC regulated 150 W quartz-halogen illuminator (PL841-1AN1, Dolan-Jenner Industries, Lawrence, MA). Dual line lights were utilized for the dual-camera system to provide evenly distributed illumination to the poultry carcasses. Alignments relative to the geometry of poultry carcass and angles of incidence are important

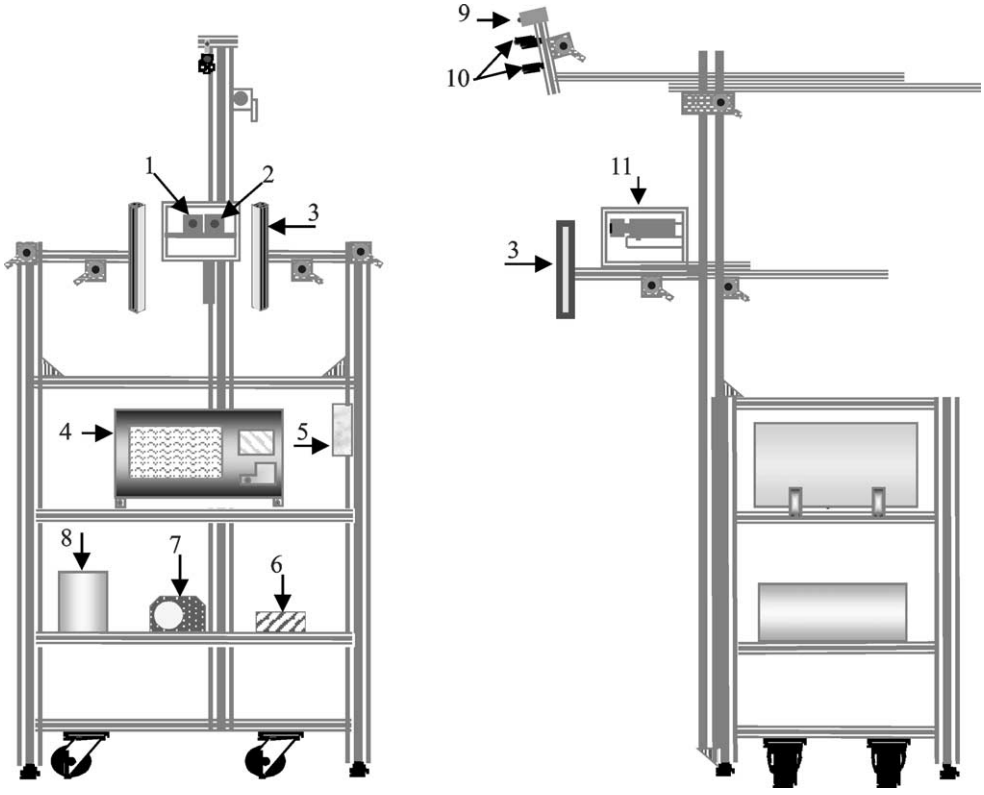

Fig. 1. Schematic of transportable dual-camera inspection system: (1) camera w/540 nm filter; (2) camera w/700 nm filter; (3) fiber-optic dual-line illuminator; (4) industrial computer; (5) interface and camera control box; (6) 12 V power supply to the dual-camera; (7) fiber-optic light source; (8) battery backup (UPS); (9) photoelectric proximity sensors; (10) magnetic proximity sensor; (11) camera enclosure.

parameters to obtain a high-quality image. Two adjustable hinges were mounted at the end of two extended profiles (arms) as pivoting joints to provide free rotation to the dual-line lights. The dual-line lights were positioned bilaterally at 45° angles to provide balanced area illumination to the poultry carcass.

Fig. 2 shows the schematic of sensor interface and control circuitry for synchronizing and triggering image acquisition. For image synchronization, the frame grabber's internal timing generator was utilized to generate horizontal and vertical synchronization signals. The output signals from the frame grabber were wired via a 12-pin connector to synchronize the horizontal and vertical data lines to the dual-camera.

Image data acquisition occurs for one of two purposes: off-line model development and on-line classification. When acquiring images for off-line model development, a stainless steel plate holding a magnet is hung on each shackle suspending a chicken carcass, marking it for image acquisition and indicating the condition of the chicken. The position of the magnet (high or low) indicates whether the chicken is wholesome or unwholesome. In this mode, the veterinarian marks (by hanging the appropriate magnetic markers) those chickens that provide a wide range of size and appearance within each class (wholesome and unwholesome).

When acquiring images for testing on-line classification, a photoelectric proximity sensor triggers image capture when a shackle is sensed. In this mode, images of all carcasses are captured, and the veterinarian marks only the unwholesome chickens by hanging the lower magnetic marker. This saves effort because usually only a very small percentage of the chickens are unwholesome.

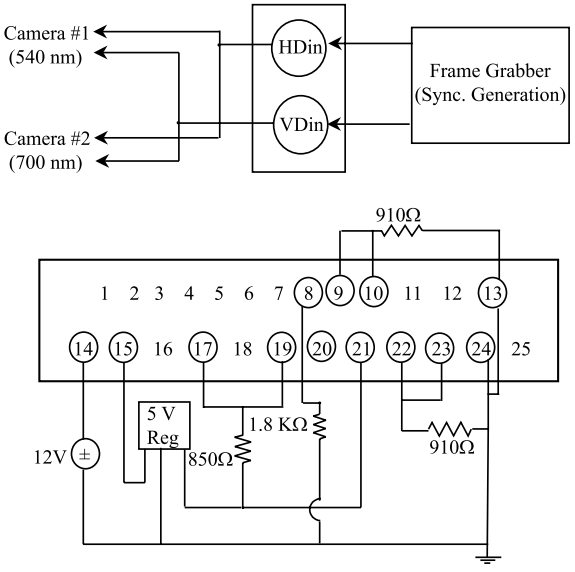

8. SS
9. Input to PIO-24 (MS #2)
10. Load (MS #2)
13. Grounding
14. Vcc
15. Power
17. Detection Output (PS)
19. Input to PIO-24 (PS)
20. Input to PIO-24 (SS)
21. Power (MS #1, #2)
22. Input to PIO-24 (MS #1)
23. Load (MS #1)

Note: HD: Horizontal Data, VD: Vertical Data, SS: Stop Switch, MS: Magnetic Switch, PS: Photoelectric Sensor.

Fig. 2. Pinout for the camera control and interface.

2.2. Software and system operation

The Machine Vision Inspection System (MVIS) was developed to integrate hardware components to provide an automated process for on-line poultry carcass inspection. Object-oriented programming paradigms (Rumbaugh, Blaha, Premerlani, Eddy, & Lorensen, 1991) were utilized to design the MVIS, and are described in detail in Chao et al., 2000. The MVIS has three primary operations: real-time imaging acquisition, processing, and on-line classification of poultry carcasses. At present in US, the viscera are still attached to the bird during inspection, hanging over the back. This configuration greatly increases the complexity of machine inspection. In these trials, only the front of the bird was imaged, to determine the utility of a simplified form of inspection.

The image processing is performed in real-time (two images per chicken, 540/700 nm). The image is reduced to a size of 256×240 pixels and then segmented from the background using simple thresholding. A total of 15 horizontal layers (16 horizontal lines of pixels each) are generated from each segmented image, as shown in Fig. 3. For each layer, a centroid is calculated from the binarized image. Based on these centroids, each layer was divided into several square blocks (16×16 pixels), for a total of 107 blocks. The averaged intensity of each block is used as the input data to the neural network models. The constant number of blocks in each layer was previously determined to delineate the main part of each carcass and omit the legs and wings. Note that for a very small chicken, the edge blocks could contain several background pixels, passing chicken size information on to the neural net in the form of lowered-average intensity.

After off-line development of the backpropagation neural network models, parameters (including weights and biases from the optimized neural network models) are saved in the ASCII data format. These parameters are then incorporated into the on-line classification section of the MVIS software. Immediately following the on-line image processing, one-pass forward mapping of the neural network application is performed to classify the carcasses as wholesome or unwholesome.

2.3. Samples and plant evaluation protocol

Chicken carcasses were measured at a processing plant in Pennsylvania over a 14-day period in September

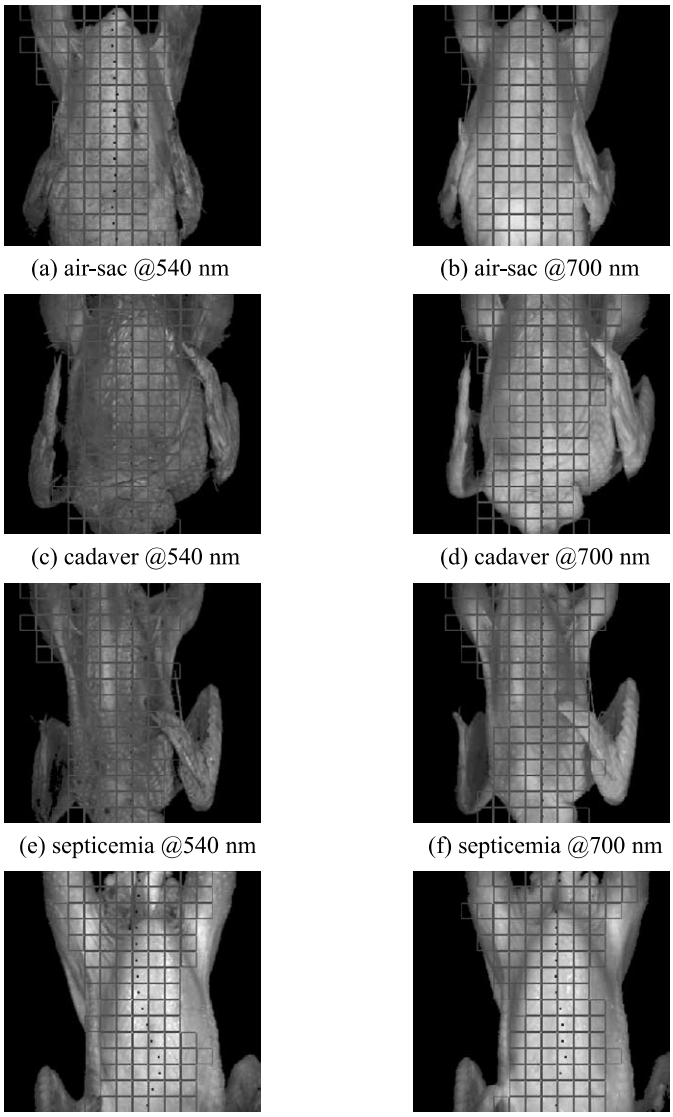

(a) air-sac @540 nm (b) air-sac @700 nm

(c) cadaver @540 nm (d) cadaver @700 nm

(e) septicemia @540 nm (f) septicemia @700 nm

(g) normal @540 nm (h) normal @700 nm

Fig. 3. Real-time multi-spectral images for poultry carcass inspection.

of 1999. The dual-camera system was installed between the evisceration station and inspector station. At this point, the chicken breasts are facing the dual-camera inspection system. Wholesome and unwholesome chicken carcasses were identified by an USDA FSIS veterinarian. Table 1 summarizes the number of carcasses that were acquired for model development and on-line testing of the inspection system. A total of 1400 poultry carcasses (700 wholesome and 700 unwholesome) were measured for development of classification models. The 'first' data set used all 1000 samples collected on or before 9/20/99. The 'second' data set used the first data set plus 300 samples (150 wholesome and 150 unwholesome) from the data collected 9/21–22/99. The 'third' data set consists of the second data set plus 100 samples (50 wholesome and 50 unwholesome) from the data collected on 9/27/99. This procedure progressively widened the variability of the calibration sets and thereby the predictive ability of the models developed from them.

Each feed-forward-back-propagation neural network is configured with 107 input nodes, 10 nodes in one hidden layer, and two output nodes. The output nodes' target outputs are (0 1) or (1 0) depending on whether the sample was identified wholesome or unwholesome by the veterinarian. For each of the three data sets, model development method starts with splitting the data into two sub-sets: training (50%) and validation (50%). Each sub-set contains equal numbers of wholesome and unwholesome carcasses. The neural network models are trained on the training sub-set. The validation sub-set is used to decide which network

Table 1
Number of carcasses used for model development and on-line testing

Date collected	Wholesome	Unwholesome	Data set	Total
Model development				
9/16/99–9/20/99	500	500	First	1000
9/21/99–9/22/99	150	150	Second	1300
9/27/99	50	50	Third	1400
Total	700	700		
On-line testing				
			Using models developed from	
9/22/99	2049	124	First data set	
9/23/99–9/24/99	4431	240	Second data set	
9/28/99–9/30/99	5952	395	Third data set	
Total	12,432	759		

Table 2
Neural network models

Model	Learning rule	Transfer function
1	Delta	Tanh
2	Delta	Sigmoid
3	Norm-cum-delta	Tanh
4	Norm-cum-delta	Sigmoid

model and how much training is optimal. The validation set is predicted every 200 iterations of the training cycle, and the network weights are saved if the classification results have been improved. Training is always stopped after 15,000 iterations.

The software used for neural network model development was NeuralWorks Professional II/Plus (NeuralWare, Pittsburgh, PA). Two back-propagation rules (delta and norm-cum-delta) and two transfer functions (sigmoid and tanh) were used for a total of four models (Table 2) for each training/validation split of the data. The models then used for on-line testing were selected based on performance on the validation set for both wholesome and unwholesome samples.

On-line testing of the inspection system was performed by neural network models previously selected from off-line training. A total of 13,191 poultry carcasses (12,432 wholesome and 759 unwholesome) were tested (Table 1). In each case, the 540 and 700 nm results were combined using an AND operation to give a single prediction. That is, a carcass is predicted wholesome only if the data from both cameras result in wholesome prediction. This prediction result and the identification result from the veterinarian were saved in ASCII files for evaluating the performance of the on-line inspection system.

3. Results and discussion

3.1. Spectral characterization of poultry carcasses

Fig. 3 shows typical images for sampled poultry carcasses at two wavelengths. Typical images of wholesome carcasses and unwholesome carcasses are shown. Septicemia is a systemic disease caused by pathogenic microorganisms in the blood. Cadaver is caused by improper slaughter cuts or inadequate bleeding time. Air-sac (airsacculitis) is commonly used to describe a respiratory syndrome.

The reflectance intensity of wholesome carcasses was not sensitive to the wavelength filters. As shown in Figs. 3(g) and (h), little difference existed in reflectance intensity between wavelengths at 500 and 700 nm. However, the reflectance intensities for unwholesome carcass at 540 and 700 nm were significantly different from that of unwholesome carcasses. For unwholesome chicken carcasses, the reflectance with the filter of the 540 nm wavelength was darker than the intensity with a 700 nm filter (Figs. 3(a)–(f)). This shows that the unwholesome spectral images at the 700 nm wavelength were not the same as that of a carcass at the 540 nm wavelength. Thus, the combination of these two wavelengths enabled the differentiation of wholesome carcasses from unwholesome carcasses.

3.2. Model development accuracy of neural network models

For each of the three data sets, four neural network models were tested to select the optimum for use in subsequent on-line classification of poultry carcasses, with results shown in Tables 3–5. With some exceptions, all models and data sets showed similar results: about 95% classification accuracy for wholesome, 88% for unwholesome and 93% for combined. The 700 nm result was slightly less accurate than that of the 540 nm for unwholesome. We suspect that this is because the more useful information is contained in the myoglobin absorbing area near 540 nm. Other research at ISL (Liu, Chen, & Ozaki, 2000) indicates that the 540 nm area is more spectroscopically sensitive to changes in the state of chicken carcasses.

There was some improvement from adding the 300 samples to the first data set to form the second data set,

Table 3
Fraction predicted correctly during off-line training using the first data set

	Wholesome carcasses	Unwholesome carcasses	All carcasses	
Carcass spectral images at 540 nm				
Model 1[a]	0.94	0.90	0.92	Training
	0.94	**0.84**	**0.89**	Validation
Model 2	0.96	0.90	0.93	Training
	0.96	0.81	0.89	Validation
Model 3	0.92	0.85	0.89	Training
	0.91	0.78	0.85	Validation
Model 4	0.95	0.87	0.91	Training
	0.94	0.80	0.87	Validation
Carcass spectral images at 700 nm				
Model 1[a]	0.95	0.81	0.88	Training
	0.95	**0.80**	**0.88**	Validation
Model 2	0.96	0.81	0.89	Training
	0.94	0.78	0.86	Validation
Model 3	0.94	0.80	0.87	Training
	0.93	0.73	0.83	Validation
Model 4	0.94	0.84	0.89	Training
	0.92	0.75	0.84	Validation

[a] Used in on-line testing.

Table 4
Fraction predicted correctly during off-line training using the second data set

	Wholesome carcasses	Unwholesome carcasses	All carcasses	
Carcass spectral images at 540 nm				
Model 1	0.95	0.91	0.93	Training
	0.96	0.85	0.90	Validation
Model 2[a]	0.94	0.94	0.94	Training
	0.94	**0.88**	**0.91**	Validation
Model 3	0.91	0.94	0.92	Training
	0.92	0.88	0.90	Validation
Model 4	0.96	0.89	0.93	Training
	0.97	0.84	0.90	Validation
Carcass spectral images at 700 nm				
Model 1	0.96	0.86	0.91	Training
	0.94	**0.88**	**0.91**	Validation
Model 2[a]	0.97	0.83	0.90	Training
	0.95	0.86	0.91	Validation
Model 3	0.98	0.78	0.88	Training
	0.99	0.81	0.90	Validation
Model 4	0.94	0.84	0.89	Training
	0.94	0.86	0.90	Validation

[a] Used in on-line testing.

but little when adding the last 100 samples to make the third data set. This indicates that during the time of the experiment, 1300 samples was sufficient to define the variability. It is probable that more data would need to be added in a longer-term test, when new populations of chickens (different breeds, feeding regimens, seasons, etc.) are encountered.

As in previous work (Chao et al., 2000), there were no striking differences between the models. We suspect it is because both transfer functions are similarly shaped in the range used. Models 1 and 2 were consistently better than 3 and 4, indicating some advantage to the simpler delta learning rule. We know of no way to test for statistical significance of these differences because such tests have not been developed for neural network results. Our choice of the model to use in subsequent online testing is based on the validation performance on 'all carcasses', with ties going to model 1. Thus, we used model 1 throughout for the 700 nm data; and we used model 2 for the 540 nm data, except for the first data set, where the slightly better performance on the unwholesome carcasses prompted a decision for model 1.

Table 5
Fraction predicted correctly during off-line training using the third data set

	Wholesome carcasses	Unwholesome carcasses	All carcasses	
Carcass spectral images at 540 nm				
Model 1	0.95	0.94	0.94	Training
	0.93	0.89	0.91	Validation
Model 2[a]	0.94	0.94	0.94	Training
	0.94	**0.89**	**0.92**	Validation
Model 3	0.94	0.93	0.93	Training
	0.95	0.87	0.91	Validation
Model 4	0.97	0.90	0.93	Training
	0.97	0.84	0.91	Validation
Carcass spectral images at 700 nm				
Model 1	0.96	0.87	0.91	Training
	0.95	**0.87**	**0.91**	Validation
Model 2[a]	0.93	0.86	0.90	Training
	0.92	0.82	0.87	Validation
Model 3	0.96	0.80	0.88	Training
	0.95	0.83	0.89	Validation
Model 4	0.94	0.89	0.91	Training
	0.90	0.88	0.89	Validation

[a] Used in on-line testing.

Table 6
Classification accuracy for on-line testing

Test on day(s)		Predicted			
			Wholesome	Unwholesome	Accuracy(%)
9/22/99	Actual	Wholesome	1864	185	90.9
		Unwholesome	22	102	82.2
9/23/99–9/24/99	Actual	Wholesome	4126	305	93.1
		Unwholesome	34	206	85.8
9/28/99–9/30/99	Actual	Wholesome	5599	353	94.0
		Unwholesome	50	345	87.3

3.3. On-line classification of unwholesome from wholesome carcasses

Table 6 shows the on-line classification results using the six best models discussed above. As stated above, the 540 and 700 nm results were combined using an AND operation to give a single prediction. This gave three sets of results, the first when the models developed from the first data set were tested on-line on 9/22/99, the second when the models developed from the second data set were tested on-line on 9/23/99, and the third when the models developed from the third data set were tested on-line on 9/28/99.

In each case, the results for the wholesome was better than that for the unwholesome, as was seen in the model development stage. The results improved from sets 1 to 2 as in model development. They also improved from set 2 to 3, indicating that the expansion of the variability in the model development sets was more than could be detected at the model development stage. We would expect the on-line testing results to be less accurate as those for training, partly because that is usually the case in a training/testing situation, and partly because of the use of the AND function. But in the third trial, the results for the wholesome improved to the 94% classification accuracy of the training stage and the unwholesome classification reached the 87% classification accuracy of the training stage. This shows that the broadening of the variability in the third training set was useful in on-line predicting, even though it was not detected in the training stage.

The success rates achieved here are not quite sufficient for a completely automated inspection system. The utility of this system would be in the high-speed screening of carcasses into two categories: a high percentage that can be processed without further inspection, and a smaller group that would need evaluation by human inspectors or machines yet to be perfected.

4. Conclusions

In previously reported results for far fewer samples run in the ISL laboratory pilot-scale facility, we obtained similar results, that is, on the order of 95% accuracy for wholesome, and 88% for unwholesome. This shows that

the instrument is fulfilling its promise, not only with respect to the precision of the desired measurement, but also in terms of durability in a commercial plant environment. Future research will involve the use of a common aperture camera with simultaneous capture of the same image at 2–4 wavelengths. This will allow not only more spectral information to be obtained, but will permit more complex use of the multi-spectral information, because of the complete image registration. Future research will also include imaging the back of each bird where there exists a configuration that permits this, such as the European viscera-pack-separation system.

References

Chao, K., Park, B., Chen, Y. R., Hruschka, W. R., & Wheaton, F. W. (2000). Design of a dual-camera system for poultry carcasses inspection. *Applied Engineering in Agriculture*, *16*(5), 581–587.

Chen, Y. R., & Massie, D. R. (1993). Visible/near-infrared refleceance and interactance spectroscopy for detection of abnormal poultry carcasses. *Transactions of the ASAE*, *36*(3), 863–869.

Chen, Y. R., Huffman, R. W., Park, B., & Nguyen, M. (1996). Transportable spectrophotometer system for on-line classification of poultry carcasses. *Applied Spectroscopy*, *50*(7), 910–916.

Chen, Y. R., Hruschka, W. R., & Earl, H. (2000). A chicken carcass inspection system using visible/near-infrared reflectance: in-plant trials. *Journal of Food Process Engineering*, *23*(2), 89–90.

Daley, W., Soulakos, C., Thompson, C., Millet, R. (1988). A novel application: machine vision inspection grading and parts identification of chicken parts. In: *Robots 12 and Vision '88, 6–9 June 1988, Detroit, Michigan* (Vol. 13, pp. 33–49). Dearborn, MI: Society of Manufacturing Engineers.

Liu, Y., Chen, Y. R., & Ozaki, Y. (2000). Characterization of visible spectral intensity variations by two-dimensional correlation spectroscopy. *Applied Spectroscopy*, *54*(4), 587–594.

OSHA. (1999). Chicken disassembly ergonomic considerations.http://www.oshaslc.gov/SLTC/poultryprocessing. US Department of Labor, Washington, DC.

Park, B., & Chen, Y. R. (1994). Intensified multispectral imaging system for poultry carcasses inspection. *Transactions of the ASAE*, *37*(6), 1983–1988.

Rumbaugh, J., Blaha, M., Premerlani, W., Eddy, F., & Lorensen, W. (1991). *Object-oriented modeling and design* (pp. 417–432). Englewood Cliffs, NJ: Prentice-Hall (Chapter 19).

US Department of Agriculture. (1997). *Poultry slaughter*. USDA/NASS, Washington, DC.